PTX3 promotes breast cancer cell proliferation and metastasis by regulating PKCζ

JING WU[1*], RUI YANG[2*], HAIZE GE[1], YU ZHU[1] and SHUYE LIU[1]

[1]Clinical Laboratory, Tianjin Key Laboratory of Extracorporeal Life Support for Critical Diseases, Tianjin Institute of Hepatobiliary Disease, Artificial Cell Engineering Technology Research Center, The Third Central Hospital of Tianjin, Tianjin 300170; [2]Department of Genetics, School of Basic Medical Sciences, Tianjin Medical University, Tianjin 300070, P.R. China

Abstract. Breast cancer (BC) is the most commonly diagnosed cancer in women, providing a leading cause of death from malignancy. Pentraxin 3 (PTX3) and protein kinase C ζ (PKCζ) are both known to exert important roles in the progression of multiple types of tumors, including BC. The present study aimed to explore both their interaction and their role in promoting the proliferation and metastasis of BC. The expression level of PTX3 was found to be elevated both in patients with BC and in BC cells; furthermore, it was found to be associated with lymph node metastasis in patients with BC. Knockdown of PTX3 decreased the rate of cell proliferation and the effects of a series of metastasis-associated cellular processes, including cell chemotaxis, migration, adhesion and invasion, as well as diminishing actin polymerization of the MDA-MB-231 and MCF7 BC cells, and decreasing tumor pulmonary metastasis *in vivo*. Mechanistically, PTX3 and PKCζ were found to be colocalized intracellularly, and they were co-translocated to the cell membrane upon stimulation with epidermal growth factor. Following the knockdown of PTX3, both the phosphorylation and membrane translocation of PKCζ were significantly impaired, suggesting that PTX3 regulates the activation of PKCζ. Taken together, the findings of the present study have shown that PTX3 may promote the proliferation and metastasis of BC cells through regulating PKCζ activation to enhance cell migration, cell chemotaxis, cell invasion and cell adhesion.

Introduction

In recent years, breast cancer (BC) has become the most commonly diagnosed malignant tumor in women (1), and the mortality rate ranks first among all types of female cancer worldwide (2). The current treatment methods for BC mainly comprise chemotherapy, radiotherapy, immunotherapy, targeted therapy and endocrine therapy (3). Although various assistive devices and novel targeted drugs have entered clinical practice, BC continues to be associated with a high rate of recurrence and mortality due to its distant metastasis to other organs (4), and the underlying metastatic mechanism has yet to be fully elucidated. Therefore, it is critical to identify both novel biomarkers and therapeutic targets for the treatment of BC.

Chemotaxis fulfills an important role in tumor metastasis, and is mediated by the chemoattractant epidermal growth factor (EGF) and its receptor (EGFR), which is expressed on the surface of tumor cells (5). Protein kinase Cζ (PKCζ) belongs to the atypical class of PKCs and fulfills multiple roles in different types of physiological processes and diseases (6). A previous study demonstrated that PKCζ is involved in the signaling of insulin-regulated glucose uptake (7), and it also has a role in glucose transport through regulating motor proteins (8). In addition, PKCζ was identified as a pro-inflammatory factor in the pathogenesis of steatohepatitis (9). The activation of PKCζ has also been shown to have a crucial role in respiratory syncytial virus replication and pathology (10). Moreover, PKCζ has continued to attract attention in various tumor fields. For example, it has been reported that PKCζ aggravates doxorubicin-induced cardiotoxicity via inhibiting Wnt/β-catenin signaling (11). Knockdown of PKCζ was shown to decrease tumor growth and lymphatic metastasis of prostate cancer in a mice xenograft model (12). In addition, PKCζ/ADAR2 (the RNA-editing enzyme adenosine deaminase acting on RNA 2) axis is a critical regulator of colorectal cancer metastasis, acting through modulation of the level of miR-200 (13). Moreover, PKCζ has also been identified as a downstream signaling molecule of AKT, which was shown to

Correspondence to: Dr Jing Wu or Dr Yu Zhu, Clinical Laboratory, Tianjin Key Laboratory of Extracorporeal Life Support for Critical Diseases, Tianjin Institute of Hepatobiliary Disease, Artificial Cell Engineering Technology Research Center, The Third Central Hospital of Tianjin, 83 Jintang Road, Tianjin 300170, P.R. China
E-mail: wujing-tj@outlook.com
E-mail: zhuyutj@126.com

*Contributed equally

be required for the EGF-stimulated chemotaxis and migration of human BC cells (14).

Pentraxin 3 (PTX3), also known as TNFAIP5 and tsg-14, is a member of the n-pentamer protein superfamily, which functions as a soluble recognition receptor protein produced by phagocytes and non-immune cells at the site of inflammation (15). Studies have shown that PTX3 exerts a central role in the process of mineralization (16), the natural immune response and inflammation (17,18), and also functions as a pro-angiogenic factor (19). Beyond the multifunctional roles of PTX3, its overexpression has been observed in several types of tumors, and its expression level has been shown to be associated with the degree of malignancy of tumors (20-22). Moreover, it has been shown that PTX3 is associated with stem-like features (23), and the epithelial-mesenchymal transition (EMT), migration and invasion of cancer cells (24). In addition, previous studies reported that activation of the PI3K/Akt signaling pathway led to an increase in the expression of PTX3 in head-and-neck squamous cell carcinomas (25,26). However, the specific mechanism through which PTX3 exerts a role in BC cell proliferation and metastasis remains contentious. The aim of the present study was therefore to verify whether PTX3 is an important molecule modulating BC cell proliferation and metastasis, and whether its primary role in BC cells may be exerted via the activation of PKCζ.

Materials and methods

Patient samples. The present study was approved by The Clinical Medical Research Ethical Committee of Tianjin Third Central Hospital (Tianjin, China; approval no. IRB2023-039-01) for the use of clinical biopsy specimens, and informed written consent was obtained from the patients. Tissues from a total of 60 cases of primary BC (including invasive ductal carcinoma and invasive lobular carcinoma), and 22 cases of benign breast tissues were collected from Tianjin Third Central Hospital (Tianjin, China). The inclusion criteria were as follows: i) Patients with pathological diagnosis of BC; and ii) patients who underwent radical mastectomy with no adjuvant treatment prior to and after surgery. Patients with serious heart, liver and kidney injuries, serious infections, endocrine and blood system diseases were excluded. In addition, the clinicopathological parameters of patients were all collected.

Cell culture. The human normal mammary epithelial cell line MCF-10A, the BC cell lines MDA-MB-231 and MCF7, and the embryonic kidney cell line 293T were purchased from the American Type Culture Collection. Cells were grown in Dulbecco's modified Eagle medium (DMEM; Biological Industries) supplemented with 10% Hyclone fetal bovine serum (FBS; Cytiva) at 37°C in an atmosphere of 5% CO_2.

Establishment of stably transfected cell lines. 293/293T cells (American Type Culture Collection) were transfected with the lentiviral packaging Lenti-Mix vector (pMDL, pVSVG or pRSV-Rev, 5:3:2; Thermo Fisher Scientific, Inc.) carrying specific small hairpin RNA (shRNA) targeting nucleotides to PTX3 (PTX3 shRNA) to generate stable cell lines. The sequence of the selected PTX3 shRNA oligomer was 5'-GCA TCCTGTGAGACCAATGAA-3'. The plasmid backbone was

pLVX-shRNA (Thermo Fisher Scientific, Inc.) and 12 μg lentiviral plasmid plus 12 μg Lenti-Mix were used for transfection. A third generation system was used and a MOI of ~40 was used to infect cells. Briefly, lentiviral supernatants were collected, centrifuged at 3,000 x g at 4°C for 10 min and filtered through a 0.45-μm filter. MDA-MB-231 and MCF7 cells were subsequently infected with lentiviral supernatant, incubated at 37°C overnight and selected with 1.5 μg/ml puromycin (Biosharp Life Sciences) for 14 days and maintained with 0.625 μg/ml puromycin for 7 days for use for subsequent experiments. Cells transfected with an unrelated sequence (scrambled siRNA) were used as the negative control. The sequence of the negative control siRNA is listed in Table SI.

Cell viability assay. Cell viability was estimated by Cell Counting Kit-8 (CCK-8) assay kit (Beijing Solarbio Science & Technology Co., Ltd.), according to the manufacturer's instructions. Briefly, cells from the control and shPTX3 groups were seeded in 96-well plates and cultured for different time periods (0, 1, 2, 3, 4 or 5 days). Aliquots (15 μl) of CCK-8 were subsequently added to each well and incubated at 37°C for 2 h. Finally, the absorbance was measured at 450 nm.

Wound healing assay. Briefly, cells were inoculated into a 6-well plate, and after the cells had reached 80-90% confluency, the cells were starved for 12 h and scratched evenly at the bottom of the orifice plate with a 10 μl tip. The distances of cell migration calculated by changes in the widths of the scratches were recorded at different time points (0, 3, 6, 9 or 12 h). A total of three measurements at different positions along each scratch-line were recorded using an Olympus BX53 light microscope (Olympus Corporation).

Chemotaxis assay. Briefly, the chemoattractant (EGF; PeproTech, Inc.) was loaded into the lower chamber, and cells ($5x10^5$/ml) suspended in binding medium (DMEM containing 0.1% bovine serum albumin and 25 mM Hepes) were subsequently loaded into the upper chamber (Neuro Probe Inc.). The two chambers were segregated with a 10 μm membrane (Neuro Probe Inc.) that had been pretreated with 10 μg/ml fibronectin (MilliporeSigma) at 4°C overnight. Subsequently, the chambers were incubated in an atmosphere containing 5% CO_2 at 37°C for 3 h. The filter membrane was then washed, and the attached cells were fixed and stained with trypan blue for 10 min at room temperature (RT). The number of migrating cells was counted in three separate fields under an Olympus BX53 microscope, and the chemotaxis index was calculated according to the following formula: Number of migrating cells in a chemoattractant gradient/the number of migrating cells in the control group.

Adhesion assay. After having starved the cells with serum-free medium containing 50 ng/ml EGF, the cells were first plated in 35 mm dishes containing a glass coverslip that had been coated with 10 μg/ml fibronectin overnight at 4°C, and then air-dried. Cells were allowed to attach to the coverslips for time periods of 5, 15 or 30 min, and subsequently were washed gently twice with cold PBS, prior to being fixed with 4% paraformaldehyde for 10 min at 4°C. Finally, all cells attached to each coverslip were counted with a hemocytometer under a light microscope with five random fields (magnification, x200).

Invasion assay. The upper surfaces of Transwell chambers containing polycarbonate membranes with 8-μm pores were coated with 20 μl diluted Matrigel™ (BD Biosciences) for 1 h at 37˚C. A total of lx10^5 cells were starved in serum-free medium for 3 h and subsequently added to the upper chamber, whereas the lower chamber was filled with the same medium as in the upper chamber, but with 10% FBS. After an incubation for 20 h at 37˚C, the cells remaining on the upper layer of the chambers were wiped off, whereas the cells attached to the submembrane surface were fixed with neutral formaldehyde for 10 min at 4˚C and stained with Giemsa for 10 min at 4˚C. Finally, the average numbers of invaded cells per field of view were obtained from five random fields under a light microscope.

F-actin polymerization assay. Briefly, cells were planted in 35 mm dishes overnight, pretreated with serum-free medium for 3 h and subsequently stimulated by adding 50 ng/ml EGF at 37˚C for time periods of 0, 15 sec, 30 sec, 1, 2 or 5 min. Thereafter, cells were fixed, permeabilized and stained in the dark with Molecular Probes™ Oregon Green 568 phalloidin (Thermo Fisher Scientific, Inc.) diluted in F-buffer (10 mM Hepes containing 20 mM KH_2PO_4, 5 mM EGTA and 2 mM $MgCl_2$ in Dulbecco's PBSl pH 6.8) at RT for 1 h. The bound phalloidin was extracted with methanol for 1 h, and the F-actin content was subsequently measured with a fluorescence reader at an excitation wavelength of 578 nm and an emission wavelength of 600 nm. The results were expressed as the relative F-actin content, where F-actin$^{\Delta}$t/F-actin0=(fluorescence$^{\Delta}$t mg/ml)/(fluorescence 0/mg/ml).

Western blotting assay. Cells were starved with serum-free medium for 3 h and stimulated by 50 ng/ml EGF for various time periods. The reactions were terminated and the cells washed twice with cold PBS, before subsequently being lysed in 1X SDS lysis buffer [Tris-HCl; pH 6.8; containing 62.5 mM (2%) SDS and 10% glycerol]. The protein determination method was via bicinchoninic acid assay. Equal amounts of protein (20 μg/lane) were separated by SDS-PAGE (10% gels) and blotted onto PVDF membranes (MilliporeSigma). The membranes were blocked with 5% non-fat milk for 1 h at RT and incubated overnight at 4˚C with the primary antibodies raised against β-actin (cat. no. 4967S; 1:3,000; Cell Signaling Technology), PTX3 (cat. no. ab190838; 1:3,000; Abcam), PKCζ (cat. no. 9372S; 1:3,000; Cell Signaling Technology), Akt (cat. no. 9272S; 1:3,000; Cell Signaling Technology), integrin β1 (cat. no. 4706S; 1:3,000; Cell Signaling Technology), cofilin (cat. no. 5175S; 1:3,000; Cell Signaling Technology) and their phosphorylated proteins (Cell Signaling Technology), followed by an incubation at RT with HRP-conjugated secondary antibody (cat. no. 7074S; 1:1,000; Cell Signaling Technology) for 1 h. Finally, the western blots were visualized using enhanced chemiluminescence reagents (Pierce; Thermo Fisher Scientific, Inc.) and analyzed with ImageJ 1.53a (National Institutes of Health).

Co-immunoprecipitation (IP) assay. After washing the MDA-MB-231 cells three times with cold PBS, the cells were lysed in 1 ml ice-cold cell lysis buffer (40 mM Hepes containing 120 mM NaCl, 1% Triton X-100, 10 mM pyrophosphate, 10 mM glycerophosphate, 50 mM NaF, 1.5 mM Na_3VO_4, 1 mM EDTA, 1X cocktail; pH 7.5) on ice for 30 min. Following centrifugation at 12,000 x g for 15 min at 4˚C, the supernatants were removed and precleared through the addition of 50 μl Invitrogen® protein A (Thermo Fisher Scientific, Inc.) for 1 h. Supernatants (50 μl) were immunoprecipitated using anti-PKCζ antibody (cat. no. ab59364; 1:3,000; Abcam). Finally, the immunocomplexes were captured by adding 50 ml protein A, and the immunocomplexes were then subjected to western blotting analysis, which was performed as aforementioned.

IP-mass spectrometry (IP-MS). Briefly, 293T cells were transfected with exogenous PKCζ and lysed with 1 ml ice cold cell lysis buffer (40 mM Hepes containing 120 mM NaCl, 1% Triton X 100, 10 mM pyrophosphate, 10 mM glycerophosphate, 50 mM NaF, 1.5 mM Na3VO4, 1 mM EDTA, 1X cocktail; pH 7.5) after 24 h. The supernatants were removed after centrifugation at 12,000 x g for 15 min at 4˚C and the PKCζ antibody was subsequently added to pull down the PKCζ-bound proteins. The protein determination method was use of the bicinchoninic acid assay, and 10% SDS gel electrophoresis was performed. Gels stained with Coomassie brilliant blue were decolorized with glacial acetic acid for 1 h at RT. The bands on the gel were then visualized and finally, proteins interacting with PKCζ were identified by LTQ-orbitrap XL MS (Thermo Fisher Scientific, Inc.). The LTQ Orbitrap XL MS was set for continuous monitoring of positive ions, and data were collected over 15 min in centroid mode over the mass range 50-1,000 m/z. The nitrogen gas temperature was set 350˚C, and cone voltage was 150 V, 30 arb of flow rate.

Immunofluorescence confocal microscopy. Briefly, MDA-MB-231 cells were plated in 12-well plates containing sterile coverslips and incubated for 24 h at 37˚C. Cells were subsequently fixed with 4% paraformaldehyde, quenched with 50 mM NH_4Cl, permeabilized with 0.2% Triton X-100 in PBS and blocked with 3% bovine serum albumin (AbMole Bioscience, Inc.). Cells were incubated with anti-PTX3 (cat. no. ab190838; 1:3,000; Abcam) and anti-PKCζ (cat. no. AB59364; 1:3,000; Abcam) antibodies overnight and stained with Invitrogen™ Alexa-Fluor 488 (cat. no. S11223; 1:3,000) and 594 (cat. no. S11227; 1:3,000) conjugated secondary antibodies for 1 h at 4˚C (Thermo Fisher Scientific, Inc.). Finally, coverslips were mounted and visualized using a confocal microscope (Nikon A1R; x400 magnification).

Immunohistochemical analysis. Paraffin tissue sections (5 μm in thickness) were firstly fixed with 4% paraformaldehyde for 12 h at 4˚C, then deparaffinized, rehydrated through graded alcohol solution and subsequently boiled (100±5˚C) in 10 mM sodium citrate for 3 min in an autoclave, followed by subsequent cooling to RT for antigen retrieval. After that, the tissues were treated with 3% hydrogen peroxide and blocked with 2% BSA for non-specific antigenic sites for 1 h at RT. The sections were subsequently incubated with the primary antibody against PTX3 (cat. no. ab190838; 1:500; Abcam) overnight at 4˚C. After washing three times with PBS, sections were incubated with the peroxidase-labeled secondary antibody (cat. no. TA373083L; OriGene Technologies, Inc.) for 30 min at RT. The reactions were visualized using an HRP DAB

Detection Kit (OriGene Technologies, Inc.), with subsequent counterstaining with hematoxylin for 5 min at RT. The images of stained sections were captured under an optical microscope, and subsequently evaluated by three experienced pathologists. The results of staining were scored as follows: 0 points, unstained; 1 point, light brown; 2 points, brown; and 3 points, dark brown. Scores ≥1 point were considered to represent positive staining.

Xenograft tumor growth and metastasis assay. All animal experiments were performed in accordance with the Guidelines for the Care and Use of Laboratory Animals of Nankai University (Tianjin, China; approval no. 2023-SYDWLL-000 545). Briefly, 4-6-week-old female severe combined immunodeficient (SCID) mice (weight, 15-20 g) from Wei Tong Li Hua Experimental Animal Co., Ltd. were randomly divided into two groups (n=10) with one group acting as the control group (transfected with pLKO.1-scrambled siRNA-luc), and another acting as the PTX3 knockdown group (transfected with pLKO.1-shPTX3-luc). The mice were bred and housed singly using a 12:12 reverse light-dark cycle in the SPF level Animal Experimental Laboratory of Nankai University, with the temperature of 22°C and 50% atmospheric humidity. Water and food were available *ad libitum*. Luciferase labelling of control cells and PTX3 knockdown of MDA-MB-231 cells were first performed (giving rise to MDA-MB-231-pLKO.1-scrambled siRNA-luc and MDA-MB-231-pLKO.1-shPTX3-luc cells, respectively), and $3x10^6$ cells were subsequently injected into the mammary fat pads of the SCID mice. The body weight of the mice was measured individually every 3 days, and the survival times were monitored. After 8 weeks, mice were intraperitoneally injected with luciferin (Amresco, Inc.) and live IVIS imaging was performed to detect the bioluminescence intensity of the tumors. The mice were sacrificed by cervical dislocation, after which the tumors were excised, and tumor volumes were measured. To examine spontaneous metastasis, the lungs were fixed with formalin for 12 h at 4°C, embedded in paraffin, then cut into 4- to 6-μm thick sections and stained with H&E stain for 5 min at RT. Finally, the metastatic tumor nodules were counted under a Zeiss inverted microscope.

Statistical analysis. SPSS version 20.0 software (IBM Corp.) was used for data analysis. Semi-quantification of the western blotting data was performed using ImageJ software (version 1.8; National Institutes of Health). Unpaired student's t-test and one-way ANOVA were used to determine statistical significance for comparisons of 2 and ≥2 groups, respectively. Data are shown as the mean ± SD and P<0.05 was considered to indicate a statistically significant difference. Tukey's test was applied for post-hoc comparisons.

Results

Overexpression of PTX3 is positively associated with the metastasis of clinical BC. First, the expression level of PTX3 was examined in 60 cases of invasive BC tissues (including invasive ductal carcinoma and invasive lobular carcinoma) and 22 cases of benign breast tissues by immunohistochemical analysis in order to assess the importance of PTX3 in BC. The results obtained showed that positive staining of PTX3

Table I. Expression of PTX3 in benign breast and BC tissues using immunohistochemical staining.

Group	Total, n	Positive, n
BC tissues	60	52
Benign breast tissues	22	2[a]

Statistically significant differences were indicated, [a]P<0.01. BC, breast cancer.

Table II. Association of PTX3 expression with clinicopathological parameters in patients with breast cancer.

Parameters	Total, n	Positive, n	%	P-value
Menopausal				
Premenopausal	33	21	63.6	0.228
Postmenopausal	27	13	48.1	
Tumor size, cm				
<2	25	17	68.0	0.853
≥2	35	23	65.7	
Lymph node status				
Negative	8	1	12.5	0.003
Positive	52	51	98.1	
T stage				
1-2	40	23	57.5	0.348
3-4	20	14	70.0	
p53 status				
Negative	47	29	61.7	0.862
Positive	13	9	69.2	
ER status				
Negative	15	8	53.3	0.274
Positive	45	31	68.9	
PR status				
Negative	28	17	60.7	0.142
Positive	32	25	78.1	

ER, estrogen receptor; PR, progesterone receptor.

was detected in 52 tumor samples, but only in two benign breast tissue samples (Table I), suggesting that the expression level of PTX3 is increased during tumorigenesis (Fig. 1). It is noteworthy that PKCζ is a cancer-promoting factor that is also highly expressed in BC tissues. In addition, the statistical analysis revealed that PTX3 expression was detected in 51 of 52 lymph node metastasis cases (P=0.003; Table II). However, only one tumor tissue was identified as being positive in eight cases of non-lymph node metastasis. Taken together, these results strongly suggested that upregulation of PTX3 is associated with lymph node metastasis of BC.

Knockdown of PTX3 inhibits the proliferation and migration of BC cells. The initial assumption was made that PTX3 fulfills
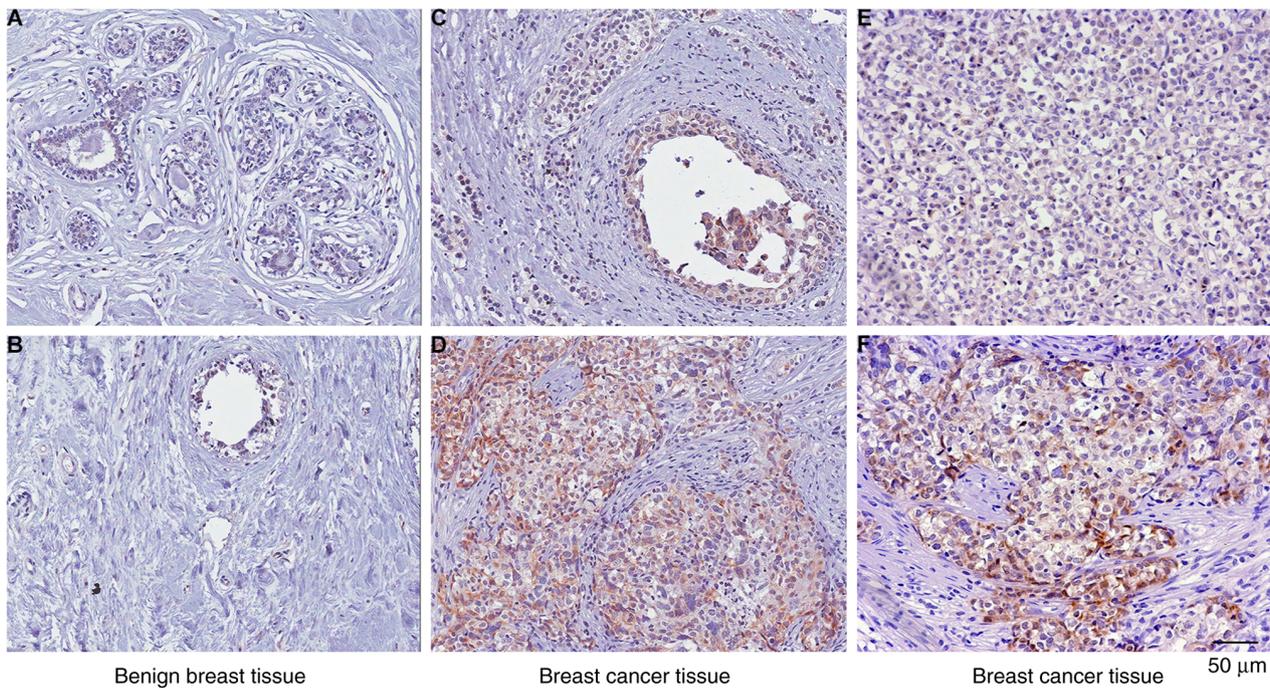
Figure 1. PTX3 expression is elevated in BC. Immunohistochemical analysis of (A and B) benign breast tissue and (C and D) BC tissues (magnification, x400). (E and F) Expression level of PKCζ in BC tissue. Sections were stained with anti-PTX3 and anti-PKCζ antibodies. PTX3, pentraxin 3; PKCζ, protein kinase Cζ; BC, breast cancer.

an important role in the proliferation and migration of BC cells. First, the expression levels of PTX3 in the human normal mammary epithelial cell line (MCF-10A) and two BC cell lines (MDA-MB-231 and MCF7) were evaluated by western blotting assay. The results obtained showed that the expression levels of PTX3 in the BC MDA-MB-231 and MCF7 cell lines were higher compared with that in MCF-10A cells (Fig. 2A), and this difference may have been associated with the malignant behavior of BC cells. Subsequently, stable PTX3 downregulation of MDA-MB-231 and MCF7 cells was performed using lentiviral packaging vectors, and the respectively transformed cells were used for the following experiments (Fig. 2B). Cell viability assay revealed that the proliferation rate of the shPTX3 cells was decreased compared with control BC cells (Fig. 2C and D). Subsequently, the migratory capability of the BC cells was examined using a wound healing assay, and changes in the scratch widths were recorded at different times. As shown in Fig. 2E and F, shPTX3-transformed cells exhibited much lower directional migratory rates compared with the control BC cells, suggesting that knockdown of PTX3 led to a marked inhibition of the migratory rate of BC cells. In addition, western blotting analysis showed a blockade at EGF-induced Akt phosphorylation at Ser473, indicating that the function of Akt was inhibited in shPTX3 cells (Fig. 2G). Taken together, the aforementioned findings revealed that knockdown of PTX3 inhibited the proliferative and migratory capabilities of the BC cells through the suppression of p-Akt expression.

Knockdown of PTX3 severely impairs the metastasis of BC cells. Subsequently, the chemotaxis of BC cells was investigated to evaluate whether PTX3 exerts a pivotal role in the metastasis of BC cells, and the results of these experiments are shown in Fig. 3A. EGF-induced chemotaxis of MDA-MB-231

and MCF7 cells was found to be markedly inhibited following PTX3 knockdown compared with the control groups (Fig. S1). As shown in Fig. 3B and D, both EGF-induced cell attachment and actin polymerization were decreased to a statistically significant extent ($P<0.05$) in shPTX3 cells compared with the control BC cells. Furthermore, PTX3 downregulation also led to a marked attenuation of the invasive capability of MDA-MB-231 and MCF7 cells compared with control cells (Fig 3C). As shown in Fig. 3E, EGF-induced phosphorylation of both cofilin and integrin β1 was severely impaired in shPTX3 cells. Taken together, these findings suggested that downregulation of PTX3 inhibits EGF-induced BC cell metastasis through inhibiting cofilin and integrin β1, which are two downstream effectors of PKCζ.

PTX3 knockdown inhibits the metastasis of BC cells through regulating PKCζ phosphorylation. The results from the MS experiments first identified PTX3 as a PKCζ-interacting protein (Fig. 4A). Therefore, it was surmised that PTX3 could regulate EGF-induced BC cell chemotaxis and metastasis through regulating the activation of PKCζ. As shown in Fig. 4B, co-IP assay confirmed that there was an interaction between PTX3 and PKCζ in MDA-MB-231 cells. Confocal microscopy analysis further revealed that both PTX3 and PKCζ were distributed in the cytosol of resting cells. Upon stimulation with 50 ng/ml EGF, however, both PTX3 and PKCζ were co-translocated to the cell membrane, suggesting the activation of proteins (Fig. 4C). The translocation of PKCζ was also analyzed in experiments that involved PTX3 knockdown of the MDA-MB-231 cells. Compared with the Scr cells, EGF-induced translocation of PKCζ was markedly inhibited in shPTX3 cells (Fig. 4D). Furthermore, according to the findings of western blotting analysis experiments, the
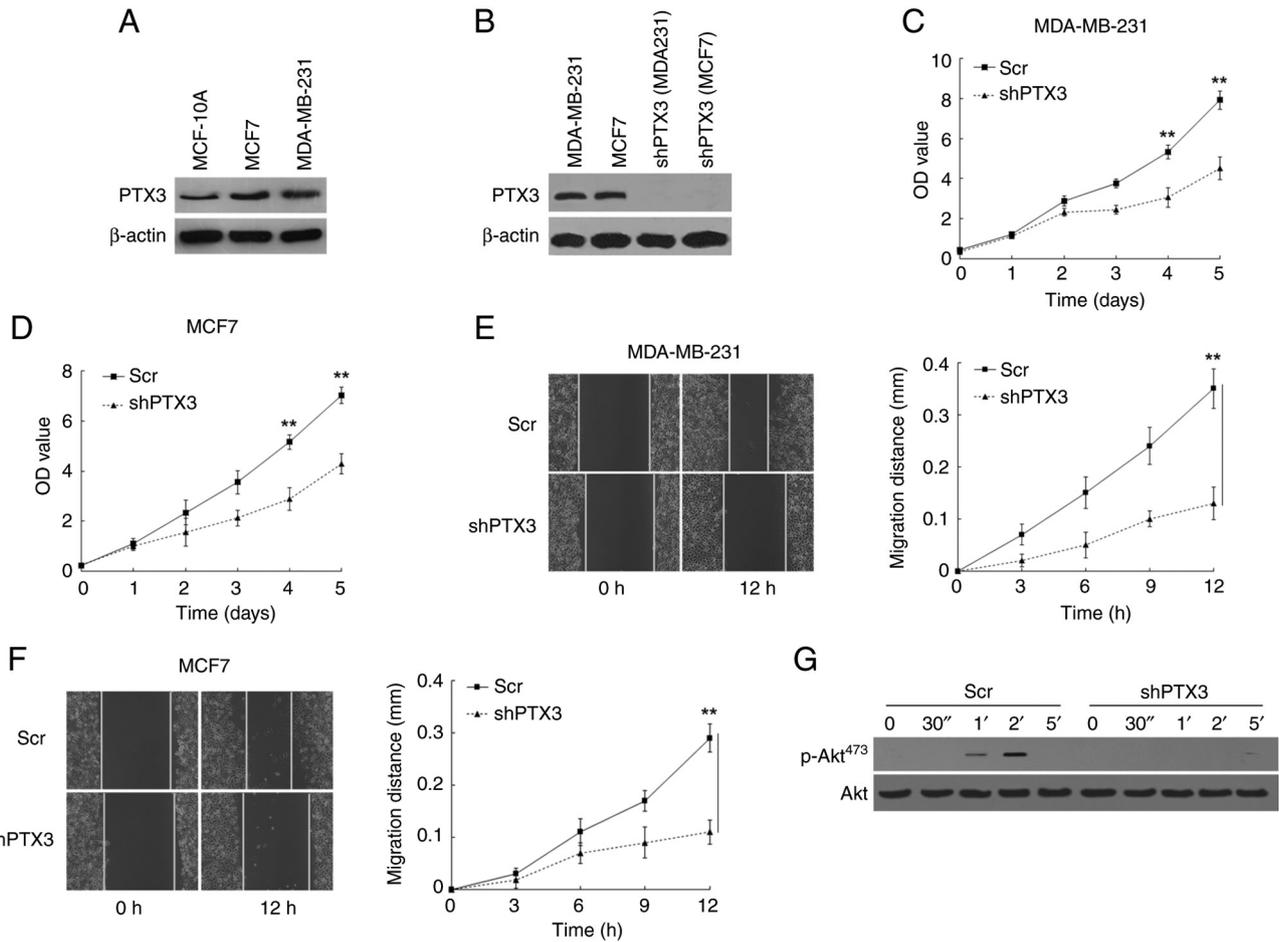
Figure 2. Knockdown of PTX3 inhibits the proliferation and migration of breast cancer cells. (A) Western blotting analysis of PTX3 protein expression in MCF-10A, MCF7 and MDA-MB-231 cells with β-actin used as a loading control. (B) Western blotting analysis of PTX3 expression in Scr and shPTX3 MDA-MB-231 and MCF7 cells with β-actin used as a loading control. (C) Proliferation assay of Scr and shPTX3 of MDA-MB-231 cells. (D) Proliferation assay of Scr and shPTX3 of MCF7 cells. (E) Wound healing assay of Scr and shPTX3 of MDA-MB-231 cells is shown (x200 magnification). The gap distance on the cell monolayer was measured at 0, 3, 6, 9 and 12 h after the scratches had been made. (F) Wound healing assay of Scr and shPTX3 of MCF7 cells (x200 magnification). (G) Western blotting analysis of EGF-induced phosphorylation of Akt at Ser^{473} in Scr and shPTX3 of MDA-MB-231 cells. Statistically significant differences are indicated with **P<0.01 according to two-way ANOVA. PTX3, pentraxin 3; EGF, epidermal growth factor; shPTX3, PTX3 stable knockdown; Scr, scrambled siRNA.

phosphorylation of PKCζ was also reduced in shPTX3 cells upon knocking down PTX3 (Fig. 4E). Taken together, these results suggested that PTX3 co-localizes with PKCζ and regulates its activation.

Knockdown of PTX3 inhibited the growth and metastasis of breast tumors. Finally, the present study aimed to explore the metastatic capabilities of shPTX3 cells in a BC xenograft model. shPTX3 and control cells were implanted into the mammary fat pads of SCID mice. After 8 weeks, the tumors were measured, and the maximum tumor size was found to be ~990 mm^3. The tumor growth in mice with transplanted shPTX3 cells was found to be markedly inhibited compared with the control group, suggesting that PTX3 exerts an important role in tumor growth *in vivo* (Fig. 5A). Subsequently, lung metastasis of the human BC cells was evaluated using H&E staining (Fig. 5B). A clear and dramatic decrease in the number of pulmonary metastatic nodules in shPTX3-implanted mice was detected compared with the control groups (Fig. 5C). Moreover, the mice with implanted shPTX3 cells also exhibited enhanced survival rates (Fig. 5D) compared with the

control mice. Therefore, these results demonstrated that PTX3 is required for the metastasis of human BCs *in vivo*, and PTX3 knockdown led to an inhibition of the growth and metastasis of breast tumors.

Discussion

BC is the second most common cause of death resulting from cancer in women (1). Both the incidence of BC and deaths resulting from BC continue to rise, and its associated mortality is mainly due to disease progression or metastasis (27). The lack of early-stage diagnostic techniques and effective treatment methods continues to present major problems for the administration of BC therapy worldwide (28). Moreover, ~6-10% of newly diagnosed cases of BC are identified at stage IV of the disease, or the BC is already metastatic (27). Therefore, there is an urgent need to explore the driving force and molecular mechanisms associated with tumor metastasis to provide novel therapeutic targets for BC.

Previous studies have shown both that PTX3 is overexpressed in various tumors, and that it is involved in cancer
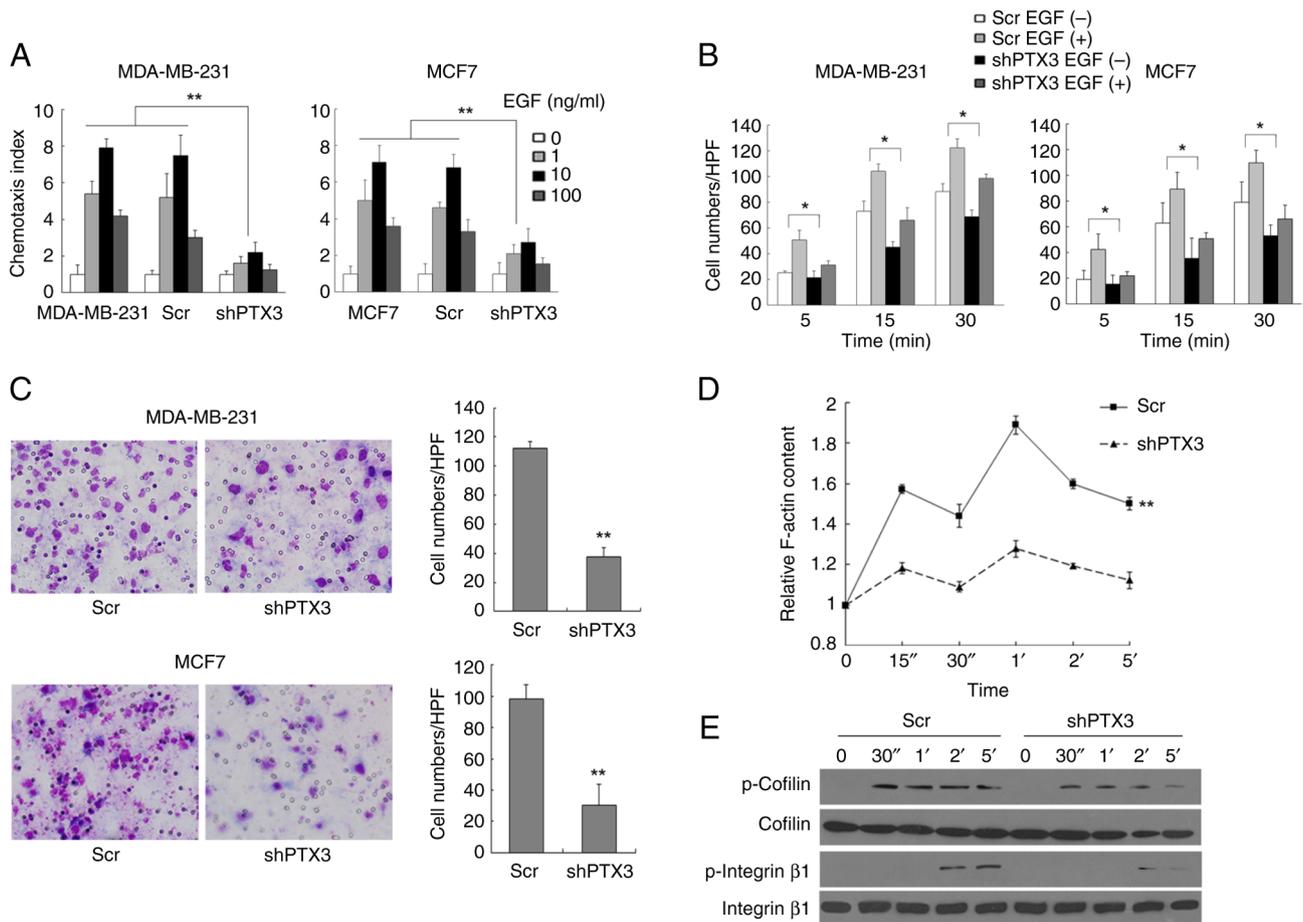
Figure 3. Knockdown of PTX3 severely impairs the metastasis of breast cancer cells. (A) EGF-induced chemotaxis of MDA-MB-231 and MCF7 cells was inhibited in shPTX3 groups. (B) EGF-induced adhesion of MDA-MB-231 and MCF7 cells was decreased in shPTX3 cells. (C) Matrigel analysis of Scr and PTX3 knockdown of MDA-MB-231 and MCF7 cells. Left: Representative images (magnification, x200) of cell invasion; right: Data presented as the mean ± SD, according to Student's t-test. (D) EGF-induced actin polymerization was decreased in shPTX3 of MDA-MB-231 cells. (E) Western blotting analysis of EGF-induced phosphorylation of cofilin and integrin β1 in Scr and shPTX3 of MDA-MB-231 cells. $^*P<0.05$ and $^{**}P<0.01$. PTX3, pentraxin 3; EGF, epidermal growth factor; shPTX3, PTX3 stable knockdown; Scr, scrambled siRNA.

progression through multiple signaling pathways (28,29). A recently published study (30) demonstrated that the transcription factor SOX9 directly regulates the expression of PTX3, whereas human leukocyte antigen system-associated genes are significantly upregulated when PTX3 is lacking in esophageal carcinoma (ESCA). Knockout of PTX3 in ESCA was also demonstrated to lead to increases in cell apoptosis and sensitivity to chemotherapy and radiotherapy (30). In addition, PTX3 expression was shown to be markedly increased in prostate cancer tissues, and PTX3 exerts an important pathogenic role in the development of prostate cancer through its ability to function as a modulator of complement activation, promoting cellular proliferation, angiogenesis and insensitivity to apoptosis, thereby leading to cancer cell invasion and migration (31). It has also been preliminarily shown that serum PTX3 may be a potential biomarker to predict the risk of prostate cancer in patients scheduled for prostate biopsy (32).

It has been shown that PTX3 is associated with tumor metastasis (33). In hepatocellular carcinoma (HCC), PTX3 expression is markedly upregulated, and its ectopic expression has been shown to enhance the migratory and invasive capabilities of HCC cells, thereby inducing an EMT phenotype (33). PTX3 has also been identified as a potential predictive factor of

poor prognosis for HCC (33). In addition, PTX3 has also been shown to be overexpressed in ovarian epithelial cancer and is strongly associated with the poor prognosis of patients with ovarian epithelial cancer (34). Moreover, it has reported that the expression level of PTX3 is higher in pancreatic ductal adenocarcinoma, and PTX3 organizes hyaluronan in conjunction with tumor necrosis factor-stimulated gene 6, thereby facilitating stellate and cancer cell invasion (35). In patients with glioma, a higher expression level of PTX3 was found to be associated with aggressive tumor behavior and shorter survival times (36). In the present study, it was observed that the expression level of PTX3 was increased both in patients with BC and in BC cells. Pathological investigation of the patient tissues revealed that a high expression of PTX3 was associated with lymph node metastasis of BC. The data obtained *in vitro* also showed that the downregulation of PTX3 led to decreased rates of BC cell proliferation, migration, chemotaxis, adhesion and invasion, and actin polymerization. In the *in vivo* animal experiments, downregulation of PTX3 was found to inhibit the metastasis of BC cells to the lungs of SCID mice, thereby providing molecular evidence that PTX3 exerts a critical role in BC cell metastasis.

As an atypical PKC isoform, PKCζ has been implicated in various types of cancer, including BC, bladder cancer, colon
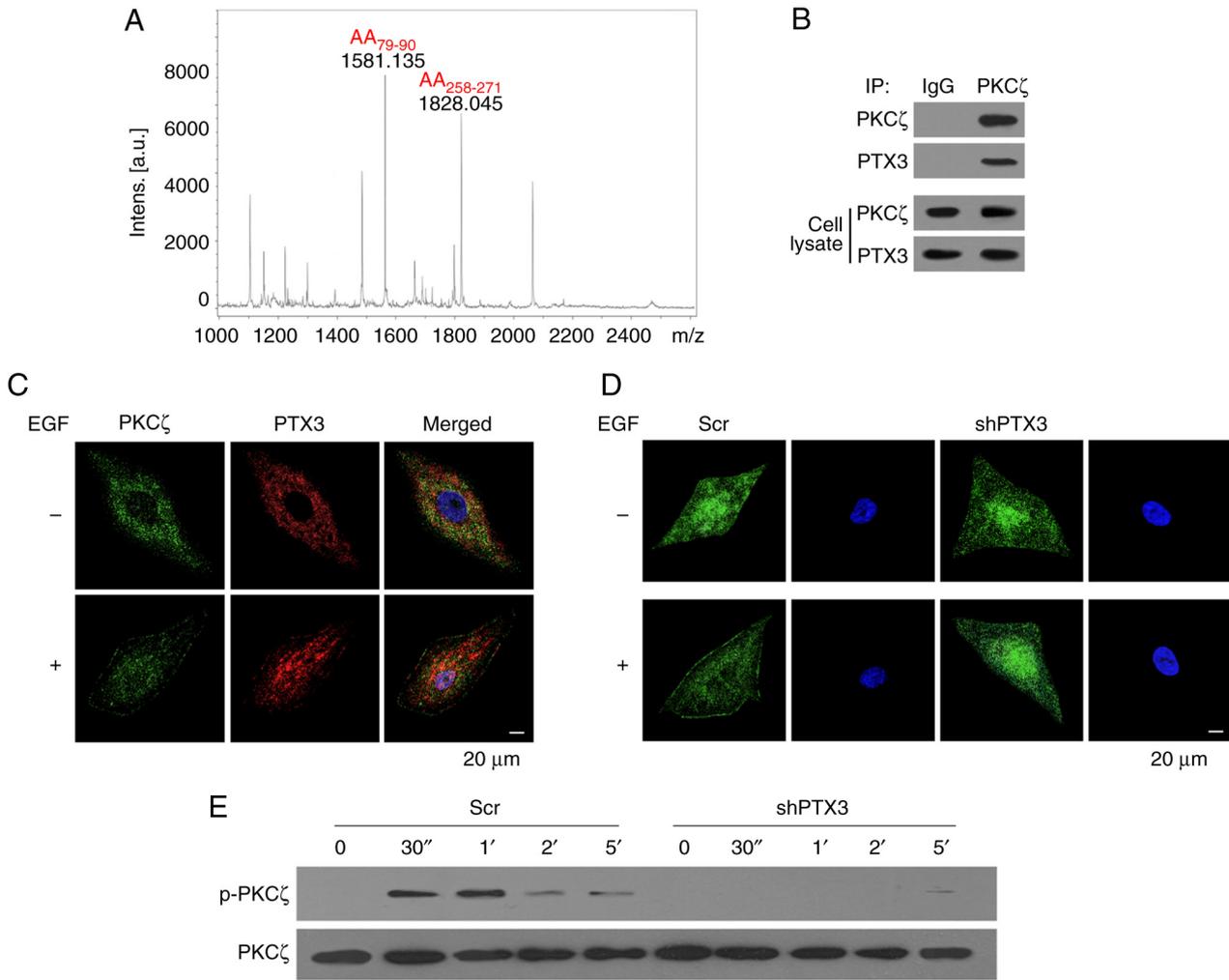
Figure 4. PTX3 is co-localized with PKCζ and regulates its activation. (A) PTX3 was identified as a PKCζ-interacting protein via mass spectrometry. (B) Co-immunoprecipitation of endogenous PTX3 or PKCζ in MDA-MB-231 cell lysates. Non-immune IgG was used as a control. (C) Co-translocation of PTX3 and PKCζ to the cell membrane following EGF stimulation was observed by confocal microscopy experiments. (D) Knockdown of PTX3 impaired EGF-induced membrane translocation of PKCζ. (E) Western blotting analysis of EGF-induced phosphorylation of PKCζ in total cell lysates from Scr and shPTX3 of MDA-MB-231 cells. PTX3, pentraxin 3; PKCζ, protein kinase Cζ; EGF, epidermal growth factor; shPTX3, PTX3 stable knockdown; Scr, scrambled siRNA.

cancer and ovarian cancer (37,38). It has been suggested that PKCζ participates in regulation of the proliferation and invasion of different types of ovarian cancer (39). Additionally, PKCζ has been shown to have an important role in the cell viability, migration and progression of bladder cancer (40). Cell adhesion and cytoskeleton rearrangement are both key responses that are closely associated with chemotaxis, and which are often regulated by PKCζ activity (41). Cofilin, as a protein associated with actin, is one of the core regulatory factors of actin polymerization (42), and integrin β1 has also been demonstrated to be involved in regulating cytoskeleton rearrangement (43). Previous studies by the research group of the present study have also indicated that PKCζ is a downstream protein of AKT that is required for the EGF-induced chemotaxis of BC cells. It has been shown that p-Akt serves an important role in the migratory and survival signaling pathways of cancer cells (44). Interestingly, activation of the NF-κB-PI3K/Akt-signaling pathway was shown to promote PTX3 expression (25), as well as having a role in mediating PTX3 transcriptional responses to EGF (26). The present study has demonstrated that endogenous PTX3 both interacts with PKCζ and is co-localized with PKCζ in BC cells. Upon EGF stimulation, PTX3 and PKCζ were co-translocated to the cell membrane, whereas knockdown of PTX3 inhibited the processes of membrane translocation and full activation of PKCζ. In addition, EGF-induced phosphorylation of integrin β1 and cofilin, which may act as the downstream effectors of PKCζ-mediated chemotaxis in BC cells, was also found to be impaired in shPTX3-transfected cells. Therefore, taken together, the findings of the present study have suggested that PTX3 is an upstream regulatory molecule of PKCζ in BC cells. The mechanisms by which PTX3 contributes to BC metastasis by regulating activation as an upstream factor of PKCζ is novel and to the best of our knowledge, has never been reported on, and the relationship between PTX3 and PKCζ has been preliminarily studied in our research and requires further investigation into their underlying mechanisms and will be the direction of future work.

In conclusion, the present study has demonstrated that PTX3 promotes BC cell proliferation and metastasis through
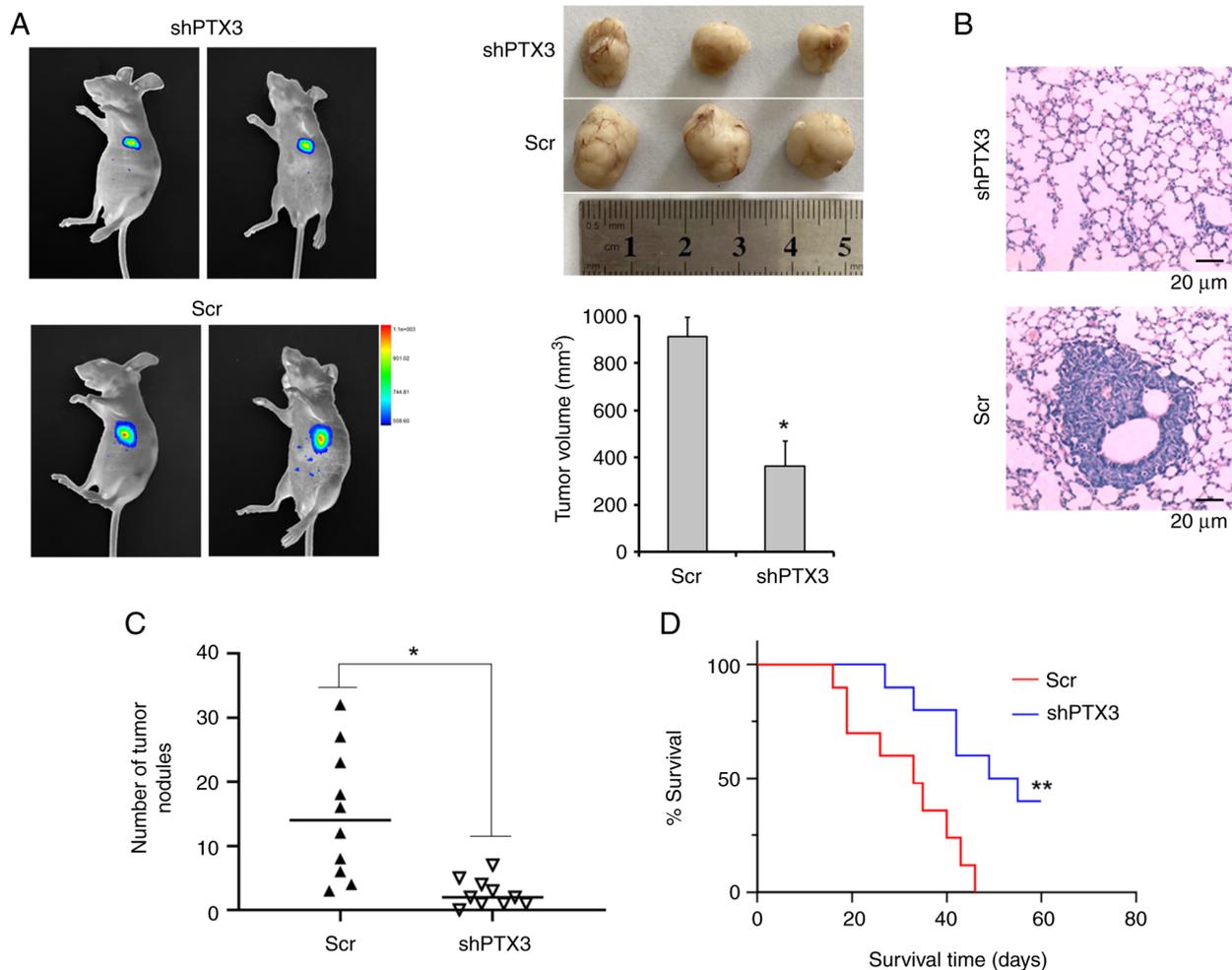
Figure 5. Knockdown of PTX3 inhibits tumor growth and metastasis of human breast tumors. (A) Comparison of tumor growth in SCID mice implanted with shPTX3-luc or Scr-luc control cells for 8 weeks. Left: Bioluminescence intensity of tumors was detected using the IVIS imaging system; right: Images of representative primary tumors and column plot of tumor volumes (bars represent the SD; *P<0.05; paired Student's t-test). (B) Comparison of spontaneous lung metastasis in SCID mice implanted with shPTX3-luc or Scr-luc control cells. The metastatic nodules on mouse lungs were visualized by H&E staining (magnification, x400). (C) Number of lung metastatic nodules was counted and plotted (n=10; *P<0.05). (D) Kaplan-Meier survival curves showing the increase in overall survival for the shPTX3 group of mice compared with controls (n=10; log-rank test; **P<0.01 vs. control). PTX3, pentraxin 3; SCID, severe combined immunodeficiency; shPTX3, PTX3 stable knockdown; Scr, scrambled siRNA.

regulating the activation of PKCζ. A high expression level of PTX3 is associated with metastasis in patients with BC, and knockdown of PTX3 was shown to effectively inhibit the proliferation, invasion and metastasis of BC cells, thereby suggesting that PTX3 may serve as a potential therapeutic target of BC. Further studies will be directed towards uncovering the underlying molecular mechanisms of PTX3 in terms of regulating PKCζ activation in BC.

Acknowledgements

Availability of data and materials

The data generated in the present study may be requested from the corresponding author.

Authors' contributions

JW and RY conceived and designed the study, and SL analyzed and interpreted the data. JW and SL wrote and edited the manuscript. JW, RY, HG and YZ performed the experiments. JW and SL confirm the authenticity of all the raw data. All authors read and approved the final version of the manuscript.

Ethics approval and consent to participate

The present study was performed in line with the principles of the Declaration of Helsinki. All animal experiments were performed in accordance with the Guidelines for the Care and Use of Laboratory Animals of Nankai University (Tianjin,

China; approval no. 2023-SYDWLL-000545). Ethics approval was obtained from The Clinical Medical Research Ethical Committee of Tianjin Third Central Hospital (Tianjin, China; approval no. IRB2023-039-01) for the use of clinical biopsy specimens and informed written consent was obtained from the patients.

Patient consent for publication

Not applicable.

Competing interests

The authors declare that they have no competing interests.

References

1. Sung H, Ferlay J, Siegel RL, Laversanne M, Soerjomataram I, Jemal A and Bray F: Global cancer statistics 2020: GLOBOCAN estimates of incidence and mortality worldwide for 36 cancers in 185 countries. CA Cancer J Clin 71: 209-249, 2021.
2. Lei S, Zheng R, Zhang S, Wang S, Chen R, Sun K, Zeng H, Zhou J and Wei W: Global patterns of breast cancer incidence and mortality: A population-based cancer registry data analysis from 2000 to 2020. Cancer Commun (Lond) 41: 1183-1194, 2021.
3. Cardoso F, Paluch-Shimon S, Senkus E, Curigliano G, Aapro MS, André F, Barrios CH, Bergh J, Bhattacharyya GS, Biganzoli L, *et al*: 5th ESO-ESMO international consensus guidelines for advanced breast cancer (ABC 5). Ann Oncol 31: 1623-1649, 2020.
4. Miller KD, Nogueira L, Mariotto AB, Rowland JH, Yabroff KR, Alfano CM, Jemal A, Kramer JL and Siegel RL: Cancer treatment and survivorship statistics, 2019. CA Cancer J Clin 69: 363-385, 2019.
5. Biswenger V, Baumann N, Jürschick J, Häckl M, Battle C, Schwarz J, Horn E and Zantl R: Characterization of EGF-guided MDA-MB-231 cell chemotaxis in vitro using a physiological and highly sensitive assay system. PLoS One 13: e0203040, 2018.
6. Dey A, Islam SMA, Patel R and Acevedo-Duncan M: The interruption of atypical PKC signaling and Temozolomide combination therapy against glioblastoma. Cell Signal 77: 109819, 2021.
7. Rosales-Soto G, Diaz-Vegas A, Casas M, Contreras-Ferrat A and Jaimovich E: Fibroblast growth factor-21 potentiates glucose transport in skeletal muscle fibers. J Mol Endocrinol 1: JME190210.R2, 2020.
8. Imamura T: The mechanisms of glucose transporter type 4 translocation regulated by insulin receptor signaling. Nihon Yakurigaku Zasshi 158: 169-172, 2023 (In Japanese).
9. Peng Y, Li JZ, You M and Murr MM: Roux-en-Y gastric bypass improves glucose homeostasis, reduces oxidative stress and inflammation in livers of obese rats and in Kupffer cells via an AMPK-dependent pathway. Surgery 162: 59-67, 2017.
10. Griffiths CD, Bilawchuk LM, McDonough JE, Jamieson KC, Elawar F, Cen Y, Duan W, Lin C, Song H, Casanova JL, *et al*: IGF1R is an entry receptor for respiratory syncytial virus. Nature 583: 615-619, 2020.
11. Cao YJ, Li JY, Wang PX, Lin ZR, Yu WJ, Zhang JG, Lu J and Liu PQ: PKC-ζ aggravates doxorubicin-induced cardiotoxicity by inhibiting Wnt/β-catenin signaling. Front Pharmacol 13: 798436, 2022.
12. Zang G, Mu Y, Gao L, Bergh A and Landström M: PKCζ facilitates lymphatic metastatic spread of prostate cancer cells in a mice xenograft model. Oncogene 38: 4215-4231, 2019.
13. Shelton PM, Duran A, Nakanishi Y, Reina-Campos M, Kasashima H, Llado V, Ma L, Campos A, García-Olmo D, García-Arranz M, *et al*: The secretion of miR-200s by a PKCζ/ADAR2 signaling axis promotes liver metastasis in colorectal cancer. Cell Rep 23: 1178-1191, 2018.
14. Wu J, Liu S, Fan Z, Zhang L, Tian Y and Yang R: A novel and selective inhibitor of PKC ζ potently inhibits human breast cancer metastasis in vitro and in mice. Tumor Biol 37: 8391-8401, 2016.
15. Nome ME, Euceda LR, Jabeen S, Debik J, Bathen TF, Giskeødegård GF, Taskén KA, Maelandsmo GM, Halvorsen B, Yndestad A, *et al*: Serum levels of inflammation-related markers and metabolites predict response to neoadjuvant chemotherapy with and without bevacizumab in breast cancers. Int J Cancer 146: 223-235, 2020.
16. Tarantino U, Greggi C, Cariati I, Visconti VV, Gasparini M, Cateni M, Gasbarra E, Botta A, Salustri A and Scimeca M: The role of PTX3 in mineralization processes and aging-related bone diseases. Front Immunol 11: 622772, 2021.
17. Netti GS, Lucarelli G, Spadaccino F, Castellano G, Gigante M, Divella C, Rocchetti MT, Rascio F, Mancini V, Stallone G, *et al*: PTX3 modulates the immunoflogosis in tumor microenvironment and is a prognostic factor for patients with clear cell renal cell carcinoma. Aging (Albany NY) 12: 7585-7602, 2020.
18. Firouzjahi A, Eris S, Jalali SF, Bijani A and Ranaee M: Evaluation of serum pentraxin-3 level in patients with acute myocardial infarction compared with control group. Iran J Pathol 16: 243-247, 2021.
19. Yadav NVS, Barcikowski A, Uehana Y, Jacobs AT and Connelly L: Breast adipocyte co-culture increases the expression of pro-angiogenic factors in macrophages. Front Oncol 10: 454, 2020.
20. Scimeca M, Antonacci C, Toschi N, Giannini E, Bonfiglio R, Buonomo CO, Pistolese CA, Tarantino U and Bonanno E: Breast osteoblast-like cells: A reliable early marker for bone metastases from breast cancer. Clin Breast Cancer 18: e659-e669, 2018.
21. Nirgude S, Desai S, Mahadeva R, Ravindran F and Choudhary B: ST08 altered NF-κB pathway in breast cancer cells in vitro as revealed by miRNA-mRNA analysis and enhanced the effect of cisplatin on tumour reduction in EAC mouse model. Front Oncol 112: 835027, 2022.
22. Chivot J, Ferrand N, Fert A, Van Dreden P, Morichon R and Sabbah M: PARP inhibitor inhibits the vasculogenic mimicry through a NF-κB-PTX3 axis signaling in breast cancer cells. Int J Mol Sci 23: 16171, 2022.
23. Zhang P, Liu Y, Lian C, Cao X, Wang Y, Li X, Cong M, Tian P, Zhang X, Wei G, *et al*: SH3RF3 promotes breast cancer stem-like properties via JNK activation and PTX3 upregulation. Nat Commun 11: 2487, 2020.
24. Kampo S, Ahmmed B, Zhou T, Owusu L, Anabah TW, Doudou NR, Kuugbee ED, Cui Y, Lu Z, Yan Q and Wen QP: Scorpion venom analgesic peptide, BMK AGAP inhibits stemness, and epithelial-mesenchymal transition by down-regulating PTX3 in breast cancer. Front Oncol 9: 21, 2019.
25. Chan SH, Tsai JP, Shen CJ, Liao YH and Chen BK: Oleate-induced PTX3 promotes head and neck squamous cell carcinoma metastasis through the up-regulation of vimentin. Oncotarget 8: 41364-41378, 2017.
26. Chang WC, Wu SL, Huang WC, Hsu JY, Chan SH, Wang JM, Tsai JP and Chen BK: PTX3 gene activation in EGF-induced head and neck cancer cell metastasis. Oncotarget 6: 7741-7757, 2015.
27. Wang X, Wang C, Guan J, Chen B, Xu L and Chen C: Progress of breast cancer basic research in China. Int J Biol Sci 17: 2069-2079, 2021.
28. Jiang J, Jiang S, Ahumada-Canale A, Chen Z, Si L, Jiang Y, Yang L and Gu Y: Breast cancer screening should embrace precision medicine: Evidence by reviewing economic evaluations in China. Adv Ther 40: 1393-1417, 2023.
29. Hu T, Qiao L, Li H, Ren H, Ning Q, Zhou H, Chen X, Sun Z and Shen L: Pentraxin 3 (PTX-3) levels in bronchoalveolar lavage fluid as a lung cancer biomarker. Dis Markers 2020: 4652483, 2020.
30. Fan Z, Zheng Y, Li X, Deng X, Ba Y, Feng K, Su J, Wang H, Suo Z and Li L: Promoting role of pentraxin-3 in esophageal squamous cell carcinoma. Mol Ther Oncolytics 24: 772-787, 2022.
31. Stallone G, Netti GS, Cormio L, Castellano G, Infante B, Pontrelli P, Divella C, Selvaggio O, Spadaccino F, Ranieri E, *et al*: Modulation of complement activation by pentraxin-3 in prostate cancer. Sci Rep 10: 18400, 2020.
32. Falagario UG, Busetto GM, Netti GS, Sanguedolce F, Selvaggio O, Infante B, Ranieri E, Stallone G, Carrieri G and Cormio L: Prospective validation of pentraxin-3 as a novel serum biomarker to predict the risk of prostate cancer in patients scheduled for prostate biopsy. Cancers (Basel) 13: 1611, 2021.
33. Song T, Wang C, Guo C, Liu Q and Zheng X: Pentraxin 3 overexpression accelerated tumor metastasis and indicated poor prognosis in hepatocellular carcinoma via driving epithelial-mesenchymal transition. J Cancer 9: 2650-2658, 2018.
34. Chang X, Li D, Liu C, Zhang Z and Wang T: Pentraxin 3 is a diagnostic and prognostic marker for ovarian epithelial cancer patients based on comprehensive bioinformatics and experiments. Cancer Cell Int 21: 193, 2021.

35. Goulart MR, Watt J, Siddiqui I, Lawlor RT, Imrali A, Hughes C, Saad A, ChinAleong J, Hurt C, Cox C, *et al*: Pentraxin 3 is a stromally-derived biomarker for detection of pancreatic ductal adenocarcinoma. NPJ Precis Oncol 5: 61, 2021.
36. Ke HH, Hueng DY and Tsai WC: Low expression of pentraxin 3 and nuclear factor-like 2 implying a relatively longer overall survival time in Gliomas. Chin J Physiol 62: 35-43, 2019.
37. Islam SMA, Patel R, Bommareddy RR, Khalid KM and Acevedo-Duncan M: The modulation of actin dynamics via atypical Protein Kinase-C activated Cofilin regulates metastasis of colorectal cancer cells. Cell Adh Migr 13: 106-120, 2019.
38. Smalley T, Islam SMA, Apostolatos C, Apostolatos A and Acevedo-Duncan M: Analysis of PKC-ζ protein levels in normal and malignant breast tissue subtypes. Oncol Lett 17: 1537-1546, 2019.
39. Smalley T, Metcalf R, Patel R, Islam SMA, Bommareddy RR and Acevedo-Duncan M: The atypical protein kinase C small molecule inhibitor ζ-Stat, and its effects on invasion through decreases in PKC-ζ protein expression. Front Oncol 10: 209, 2020.
40. Patel R, Islam SA, Bommareddy RR, Smalley T and Acevedo-Duncan M: Simultaneous inhibition of atypical protein kinase-C and mTOR impedes bladder cancer cell progression. Int J Oncol 56: 1373-1386, 2020.
41. Kay RR, Langridge P, Traynor D and Hoeller O: Changing directions in the study of chemotaxis. Nat Rev Mol Cell Biol 9: 455-463, 2008.
42. Sun R, Gao P, Chen L, Ma D, Wang J, Oppenheim JJ and Zhang N: Protein kinase C ζ is required for epidermal growth factor-induced chemotaxis of human breast cancer cells. Cancer Res 65: 1433-1441, 2005.
43. .Ghatak S, Misra S, Moreno-Rodrigue RA, Hascall VC, Leone GW and Markwald RR: Periostin/β1integrin interaction regulates p21-activated kinases in valvular interstitial cell survival and in actin cytoskeleton reorganization. Biochim Biophys Acta Gen Subj 1863: 813-829, 2019.
44. Wu YQ, Ju CL, Wang BJ and Wang RG: PABPC1L depletion inhibits proliferation and migration via blockage of AKT pathway in human colorectal cancer cells. Oncol Lett 17: 3439-3445, 2019.